Role of Protein Conformational Mobility in Enzyme Catalysis: Acylation of α-Chymotrypsin by Specific Peptide Substrates†

Alvan C. Hengge‡ and Ross L. Stein*,#,§

Department of Chemistry and Biochemistry, Utah State University, 0300 Old Main Hill, Logan, Utah 84322, and Department of Neurology, Harvard Medical School, Laboratory for Drug Discovery in Neurodegeneration, Harvard Center for Neurodegeneration and Repair, 65 Landsdowne Street, Fourth Floor, Cambridge, Massachusetts 02139

Received October 15, 2003; Revised Manuscript Received November 12, 2003

ABSTRACT: To probe the mechanistic origins of convex Eyring plots that have been observed for α-chymotrypsin (α-CT)-catalyzed hydrolysis of specific *p*-nitroanilide substrates [Case, A., and Stein, R. L. (2003) *Biochemistry 42*, 3335−3348], we determined the temperature-dependence of ^{15}N-kinetic isotope effects for the α-CT-catalyzed hydrolysis of *N*-succinyl-Phe *p*-nitroanilide (Suc-Phe-pNA). To provide an interpretational context for these enzymatic isotope effects, we also determined ^{15}N-KIE for alkaline hydrolysis of *p*-nitroacetanilide. In 0.002 and 2 N hydroxide (30°C), ^{15}N-KIE values are 1.035 and 0.995 (±0.001), respectively, and are consistent with the reported [HO^-]-dependent change in rate-limiting step from leaving group departure from an anionic tetrahedral intermediate in dilute base, to hydroxide attack in concentrated base. For the α-CT-catalyzed hydrolysis of Suc-Phe-pNA, ^{15}N-KIE is on k_c/K_m and thus reflects structural features of transition states for all reaction steps up to and including acylation of the active site serine. The isotope effect at 35 °C is 1.014 (±0.001) and suggests that in the transition state for this reaction, departure of leaving group from the tetrahedral intermediate is well advanced. Significantly, ^{15}N-KIE does not vary over the temperature range 5−45 °C. This result eliminates one of the competing hypotheses for the convex Eyring plot observed for this reaction, that is, a temperature-dependent change in rate-limiting step within the chemical manifold of acylation, but supports a mechanism in which an isomerization of enzyme conformation is coupled to active site chemistry. We finally suggest that the near absolute temperature-independence of ^{15}N-KIE may point to a unique transition state for this process.

It has been recognized for decades now that protein conformational isomerizations must play some role in enzyme catalysis. Examination of the literature reveals at least three ways in which conformational changes of the enzyme can participate in catalysis: (i) allowing the binding of substrate or departure of product, (ii) preorganizing active site residues for optimal interaction with substrates, and (iii) directly reducing activation energy by coupling to active site chemistry in catalytic transition states. In a recent study, Case and Stein (*1*) reported evidence supporting the third hypothesis for reactions of α-chymotrypsin (α-CT),[1] a well-studied member of the family of serine proteases.

Scheme 1: Minimal Kinetic Mechanism for Serine Protease Catalysis

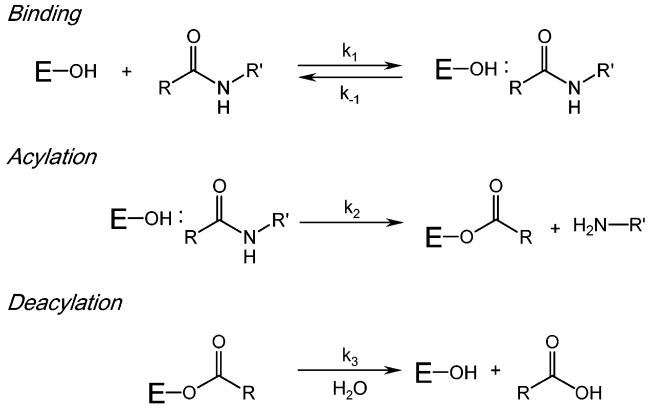

Serine proteases catalyze the hydrolysis of amide bonds of their protein and peptide substrates according to the three-step mechanism of Scheme 1. In the first step, substrate and enzyme combine to form the Michaelis complex. From within this complex, the hydroxyl of the active site serine attacks the carbonyl carbon of the amide bond of the substrate to generate an acyl-enzyme intermediate and liberate the first product. Finally, hydrolysis of the acyl-enzyme produces the

† Portions of this work were supported by NIH Grant (GM47297) awarded to A.C.H.

* To whom correspondence should be addressed at Laboratory for Drug Discovery in Neurodegeneration, Harvard Center for Neurodegeneration and Repair, 65 Landsdowne Street, Fourth Floor, Cambridge, MA 02139. Phone: (617) 768−8651. Fax: (617) 768−8606. E-mail: rstein@rics.bwh.harvard.edu.

‡ Department of Chemistry and Biochemistry, Utah State University.

Department of Neurology, Harvard Medical School,

§ Laboratory for Drug Discovery in Neurodegeneration, Harvard Center for Neurodegeneration and Repair.

[1] Abbreviations: Suc, *N*-succinyl; pNA, *p*-nitroanilide; PNAA, *p*-nitroacetanilide; α-CT, α-chrymotrypin; k_E, k_c/K_m; ^{15}k, ^{15}N-isotope effect on the rate constant *k*; e.u., entropy unit or cal/mol.

10.1021/bi030222k CCC: $27.50
Published on Web 12/31/2003

reaction's second product and regenerates free enzyme. For this mechanism, the steady-state rate parameters, k_c/K_m, k_c, and K_m, are related to the mechanistic rate parameters, K_s, k_2, and k_3, as shown in eqs 1−3.

$$\frac{k_c}{K_m} = \frac{k_2}{K_s} \quad (1)$$

$$k_c = \frac{k_2 k_3}{k_2 + k_3} \quad (2)$$

$$K_m = K_s\left(\frac{k_3}{k_2 + k_3}\right) \quad (3)$$

In these expressions, $K_s = (k_{-1} + k_2)/k_1$, which for hydrolyses of most amides can be simplified to $K_s = k_{-1}/k_1$.

In their study, Case and Stein determined the temperature-dependencies of K_s, k_2, and k_3 for the α-CT-catalyzed hydrolyses of Suc-Phe-pNA, Suc-Ala-Phe-pNA, and Suc-Ala-Ala-Pro-Phe-pNA (*1*). For reaction of all three substrates, the van't Hoff plots for $1/K_s$ and the Eyring plots for k_3 were linear, while the Eyring plots for k_2 were convex. Of the several hypotheses offered to account for the curved Eyring plots for k_2, the one that was favored posited that protein conformational isomerization was coupled to active site chemistry. A feasible competing hypothesis was also offered and involved partially rate-limiting formation and decomposition of the tetrahedral intermediate that is thought to form during acylation by amide substrates. To distinguish these hypotheses, Case and Stein proposed conducting a ^{15}N-isotope effect experiment with the anticipation of a temperature-independent ^{15}N-isotope effect, if the curved Eyring plot was due to coupling of protein motion to chemistry, or a temperature-dependent ^{15}N-isotope effect, if partially rate-limiting formation and decomposition of a tetrahedral intermediate were obtained. In this paper, we now report the results of these isotope effect experiments. $^{15}k_E$ for the acylation of α-CT by the specific substrate Suc-Phe-pNA was found to be temperature-independent and thus rules out the latter mechanism.

MATERIALS AND METHODS

General. Buffer salts, Suc-Phe-pNA, and PNAA were from Sigma Chemical Co. PNAA was recrystallized from water before use. Bovine α-CT was a crystalline product from Sigma (C 7762) and was used without further purification. Preparative TLC was performed using 20 × 20 cm silica gel GF 1000 micron plates from Analtech.

Isotope Effects for α-Chymotrypsin-Catalyzed Reaction of Suc-Phe-pNA. Suc-Phe-pNA (38.5 mg, 100 μmol) was dissolved in 35 mL of HEPES buffer (0.1 M, pH = 7.4) at 20 °C. A total of 3 mg of α-chymotrypsin was then added and the reaction was allowed to proceed for 48 h until half of the substrate had been cleaved ($[S]_o$ = 2.9 mM; $[E]_o$ = 3.3 μM). Reaction progress was accessed by periodically adding 50 μL of the reaction mixture to 3 mL of pH 9 buffer and monitoring OD_{410}. Treating an aliquot of the reaction mixture with 1 N NaOH and monitoring OD_{410} for 10 half-lives established the final OD_{410}. Control experiments showed no measurable release of *p*-nitroaniline in the absence of enzyme.

Reaction mixtures were extracted with diethyl ether 3 × 50 mL, which control experiments determined quantitatively removed *p*-nitroaniline from the aqueous layer, while leaving unreacted Suc-Phe-pNA. Ether layers were dried over $MgSO_4$ and concentrated in vacuo. The aqueous layer was made 1 N in HO^- by addition of solid NaOH and allowed to stand overnight at 25 °C, resulting in complete release of *p*-nitroaniline from the remaining Suc-Phe-pNA. *p*-Nitroaniline thus produced was isolated as described. Samples of *p*-nitroaniline representing product and unreacted substrate were purified by preparative TLC eluting with diethyl ether. The $^{15}N/^{14}N$ ratios of the samples were analyzed by isotope ratio mass spectrometry using an ANCA-NT combustion system working in tandem with a Europa 20−20 isotope ratio mass spectrometer.

Reactions at 45 °C were run on a similar scale, but ∼20 mg of enzyme ($[E]_o \sim 23$ μM) was used to achieve sufficient product formation for isotope ratio mass spectrometry before thermal inactivation of the enzyme occurred. When sufficient turnover was achieved, the reactions were cooled with ice and extracted with ether, as for the 20 °C reactions.

Alkaline Hydrolysis of p-Nitroacetanilide. PNAA (18 mg, 100 μmol) was dissolved in 6 mL of THF. This solution was added to 95 mL of 2.1 N KOH with stirring. Reaction was periodically monitored as described above for the enzymatic reactions. After 20−30 min the reaction was stopped by rapidly adjusting the pH to 9 by addition of cold HCl, and chilling the reaction mixture. The reaction was then extracted with ether (3 × 100 mL), which quantitatively removed both the *p*-nitroaniline and unreacted *p*-nitroacetanilide. The ether layers were dried over magnesium sulfate and concentrated in vacuo. Preparative TLC eluting with ether was used to separate the *p*-nitroaniline and *p*-nitroacetanilide, and samples of each were prepared for isotope ratio mass spectrometry.

For reactions at 0.002 N HO^-, CAPS buffer (10 mM, pH 11.3) was used. Higher initial amounts of reactant (28 mg, 156 μmol) were used, anticipating lower fractions of reaction due to the much slower rate of reaction at this pH. PNAA was dissolved in 6 mL of THF and added to 95 mL of buffer with stirring. Reactions were allowed to proceed at 30 °C for 5 days. The reactions were stopped by chilling with ice, and the product and remaining reactant were isolated and separated as described for the reactions run at 2 N HO^-.

RESULTS

Kinetic Isotope Effect Data Analysis. For each isotope effect, at least three reactions were run. Each reaction was stopped at some fraction of reaction *f*, and the $^{15}N/^{14}N$ ratios measured for the product (R_p), the remaining starting material (R_s), and the original mixture (R_o). The isotope effects were calculated using eqs 4 and 5 (*2*).

$$\text{isotope effect} = \log(1 - f)/\log[(1 - f)(R_s/R_o)] \quad (4)$$

$$\text{isotope effect} = \log(1 - f)/\log(1 - f(R_p/R_o)) \quad (5)$$

For each isotope effect, the value calculated from R_o and R_s (eq 4) and from R_o and R_p (eq 5) agreed within experimental error, and these were averaged to give the results reported (see Table 1).

Table 1: Nitrogen Isotope Effects for Hydrolysis of *p*-Nitroanilides

reaction system	T (°C)	$^{15}k_{obs}$	$^{15}k_{amido}$	
			$^{15}k_{nitro} =$ 1.0000	$^{15}k_{nitro} =$ 1.0023
PNAA, 2 N HO^-	30	0.9975 ± 0.0003	0.995	0.993
PNAA, 0.002 N HO^-	30	1.0173 ± 0.0003	1.035	1.033
PNAA, 0.002 N HO^-	55	1.0163 ± 0.0001	1.033	1.031
Suc-Phe-pNA, α-CT	5	1.0074 ± 0.0002	1.015	1.013
Suc-Phe-pNA, α-CT	20	1.0069 + 0.0002	1.014	1.012
Suc-Phe-pNA, α-CT	35	1.0069 ± 0.0003	1.014	1.012
Suc-Phe-pNA, α-CT	45	1.0068 ± 0.0002	1.014	1.011

The leaving group in both the reactions studied here, *p*-nitroaniline, contains two nitrogen atoms that contribute to the isotope ratio measurements and thus to the observed isotope effect, $^{15}k_{obs}$. Equation 6 relates the contribution of the isotope effects at these two sites

$$\frac{1}{^{15}k_{obs}} = \frac{(^{15}k_{amido})^{-1} + (^{15}k_{nitro})^{-1}}{2} \qquad (6)$$

to $^{15}k_{obs}$[2] (*3*). For the enzymatic reactions, the corresponding terms are $^{15}k_E$ in place of ^{15}k where k_E is k_c/K_m (*4*).

The amido nitrogen atom will exhibit a primary isotope effect, while the nitro nitrogen atom should contribute a much smaller secondary isotope effect, and only to the extent that negative charge develops on the leaving group in the transition state. An estimation for the maximum contribution of the secondary effect can be made from the behavior of the $^{15}k_{nitro}$ isotope effect in reactions involving *p*-nitrophenol. Deprotonation of *p*-nitrophenol is accompanied by $^{15}k_{nitro} =$ 1.0023, arising from negative charge delocalization involving the nitro group (*5*).

The observed isotope effects were corrected assuming $^{15}k_{nitro}$ is unity, and also assuming that $^{15}k_{nitro}$ equals its maximum expected value of 1.0023. The differences are very small and do not affect the interpretation of the results. These results are all summarized in Table 1.

DISCUSSION

The principal goal of this study was to determine ^{15}N-isotope effects at several temperatures for the α-CT-catalyzed hydrolysis of Suc-Phe-pNA and then to use this temperature dependence to distinguish among competing hypotheses that had been advanced to explain convex Eyring plots for this and related α-CT-catalyzed reactions (*1*). As a mechanistic backdrop to these studies, we first describe ^{15}N-isotope effects on the alkaline hydrolysis of PNAA (see Table 1) as well as several literature studies of ^{15}N-isotope effects for mechanistically related systems.

^{15}N-Isotope Effects for Hydrolysis of Amides and Anilides. Alkaline Hydrolysis of p-Nitroacetanilide. In this study, we determined ^{15}N-isotope effects for alkaline hydrolysis of PNAA and found that at 0.002 N HO^-, $^{15}k_{amido} = 1.035$, while at 2 N HO^-, $^{15}k_{amido} = 0.995$ (see Table 1). These results are consistent with a previous study of this reaction that showed that at 0.002 N HO^-, decomposition of a tetrahedral adduct formed from addition of hydroxide to PNAA is rate determining, while at 2 N HO^-, nucleophilic attack by hydroxide becomes rate determining (*6*). Thus, we see that the large normal effect for $[HO^-] = 0.002$ N reflects decomposition of the tetrahedral intermediate and results primarily from a weakening of the stretching force constant during C−N bond rupture. The observed value of 1.035 is close to the theoretical maximum of 1.044 that has been calculated for breaking a C−N bond (*7*). In contrast, the small inverse isotope effect at 2 N HO^- reflects adduct formation and most likely results from the hybridization change of the carbonyl carbon from sp^2 toward sp^3. For this reaction, $^{15}k_{amido}$ is a secondary KIE resulting from isotopic substitution at a position adjacent to a carbon atom undergoing a change in hybridization and is predicted to be inverse due to compression of bending modes (*8*). Apparently, this effect is more pronounced than the reduction in C−N bond order from loss of amide resonance, which would result in a normal isotope effect.

Enzymatic Hydrolysis of Amides and Anilides. Several pertinent measurements of nitrogen isotope effects on the enzymatic hydrolysis of amides and anilides have been reported. $^{15}k_E$ for the α-CT-catalyzed hydrolysis of *N*-acetyl-L-tryptophanamide (*9*) and the papain-catalyzed hydrolysis of *N*-benzoyl-L-argininamide (*10*) are 1.010 ± 0.001 and 1.021 ± 0.001, respectively (pH 8, 25 °C). While the latter was interpreted as perhaps reflecting rate-limiting decomposition of the tetrahedral intermediate that is formed from attack of papain's active site cysteine on substrate, the former was thought to result from a situation in which both formation and decomposition of the tetrahedral intermediate are partially rate limiting. Even in cases where C−N bond fission is entirely rate limiting, nitrogen isotope effects are anticipated to be smaller than the theoretical maximum of 1.044 due to protonation of the departing amine (*11*).

In another study, the ^{15}N-isotope effect was determined for the acetylcholinesterase-catalyzed hydrolysis of *o*-nitroacetanilide (*3*) and found to be 1.0119 ± 0.0005. In addition, the authors also observed a solvent deuterium isotope effect on k_E of 1.6 ± 0.1 and a small but real solvent deuterium isotope effect on the ^{15}N-isotope effect. Combined, these data led the authors to conclude that acylation of AChE by ONAA is partially rate-limited by three serial steps: induced-fit binding of substrate, formation of a tetrahedral intermediate, and decomposition the tetrahedral intermediate.

Theoretical Considerations for ^{15}N-Isotope Effects on Serine Hydrolases. The ^{15}N-isotope effects that we report here for the α-CT-catalyzed hydrolysis of Suc-Phe-pNA, and those reported elsewhere in the literature for related hydrolytic enzymes (see above), were all determined by competitive methods relying on the natural abundance of ^{15}N. In such experiments, the measured isotope effect must necessarily be on k_E and thus reflects all reaction steps up to and including the first irreversible step. For α-CT and mechanistically related cysteine and serine hydrolases, this step is acylation by substrate of active site nucleophile (i.e., k_2 of Scheme 1).

Now, a key mechanistic feature of all these enzymes is that acylation proceeds through a tetrahedral addition adduct. The inclusion of this tetrahedral intermediate into the general

[2] Implicit in this equation is the assumption that the initial $^{15}N/^{14}N$ ratios at the two position unit or cal/mol.

Scheme 2: Expanded Mechanism for Serine Protease Catalysis Including Intermediacy of Tetrahedral Addition Adduct TI

mechanism is shown in Scheme 2. The kinetic expressions of eqs 1−3 still hold but now

$$k_2 = \frac{k_{2a}}{1 + \alpha} \tag{7}$$

and

$$k_E = \frac{k_1 k_{2a}}{k_{-1}(1 + \alpha) + k_{2a}} \tag{8}$$

where

$$\alpha = \frac{k_{-2a}}{k_{2b}} \tag{9}$$

Equations 7 and 8 were expressed as shown here to intentionally center attention on the tetrahedral intermediate and how its partitioning, as reflected in the ratio α, determines rate limitation for the overall process of acylation.

For sequential reactions, such as the one shown Scheme 2, it has been shown (*12*) that the observed isotope effect has the general form:

$$^{x}k_{obs} = \sum_{i=1}^{n} C_i {}^{x}k_i^* \tag{10}$$

where *x* is the isotope for which the kinetic effect is being determined, $^{x}k_{obs}$ is the observed *x*-isotope effect, *n* is the number of sequential steps in the reaction, $^{x}k_i^*$ is the *x*-isotope effect on the reaction process that is governed by k_i^*, and C_i is a weighting factor for the *i*th step.

k_i^* reflects the free energy difference between the reactant state of enzyme and substrate free in solution and the transition state for k_i. k_i^* is a composite rate constant and will be a function of all the mechanistic rate constants that "connect" the reactant state to the transition state for k_i. For sequential reactions, k_i^* has the following form:

$$k_i^* = \left(\prod_{j=1}^{j=(i-1)} \frac{k_j}{k_{-j}} \right) k_i \tag{11}$$

where *j* denotes the several steps preceding and leading to reaction step *i*.

C_i is the weighting factor for the contribution of the *i*th step to rate determination of the overall process and thus also for the weighting factor for the contribution of the isotope effect on the *i*th step to determining the magnitude of the overall isotope effect. For sequential reactions,

$$C_i = \frac{k_{obs}}{k_i^*} \tag{12}$$

where k_{obs} is the observed rate constant for the reaction process under question.

Applying the eqs 10−12 to the ^{15}N-isotope effect for the mechanism of Scheme 2 we see that

$$^{15}k_E = C_1(^{15}k_1) + C_{2a}(^{15}k_{2a}^*) + C_{2b}(^{15}k_{2b}^*) \tag{13}$$

where

$$C_1 = \frac{k_E}{k_1} \tag{14}$$

$$C_{2a} = \frac{k_E}{k_{2a}^*} \tag{15}$$

$$C_{2b} = \frac{k_E}{k_{2b}^*} \tag{16}$$

Equation 13 can be simplified to eq 17 if we make the reasonable assumptions that both $^{15}k_1$ and $^{15}k_{2a}^*$ have values near unity and C_1 is very nearly zero (i.e., $k_1 \gg k_E$):

$$^{15}k_E = C_{2a} + C_{2b}(^{15}k_{2b}^*) \tag{17}$$

Note that under this circumstance, C_{2a} and C_{2b} simplify to $1/(1 + \alpha)$ and $\alpha/(1 + \alpha)$, respectively, and since $\sum C_i$ always equals unity, the sum of C_{2a} plus C_{2b} must equal one.

We see then that in cases in which formation of the tetrahedral intermediate is entirely rate limiting (i.e., $\alpha \ll 1$) and C_{2a} equals 1, the observed isotope effect will equal 1 (or perhaps be slightly inverse), while for those cases in which decomposition of the tetrahedral intermediate is entirely rate limiting (i.e., $\alpha \gg 1$) and C_{2b} equals 1, the observed isotope effect will equal $^{15}k_{2b}$, which can range from 1.01 to 1.04 (*3*, *9*, *10*, *13*). For intermediate situations in which formation and decomposition of the tetrahedral intermediate are both partially rate limiting, a virtual transition state (*12*) will be observed and will generate an isotope effect that is of intermediate magnitude.

^{15}N-Isotope Effects for αCT-Catalyzed Hydrolysis of Suc-Phe-pNA. $(^{15}k_E)_{amido}$ for the α-CT-catalyzed hydrolysis of Suc-Phe-pNA is 1.014, and, given a maximum ^{15}N-isotope effect on C−N bond fission of about 1.044, it suggests that the process governed by k_E is at least partially rate limited by departure of leaving group *p*-nitroaniline from the tetrahedral intermediate. Indeed, it may be the case that leaving group expulsion entirely rate limits k_E, in light of the general-acid catalysis that likely accompanies this step and the damping effect that general catalysis is anticipated to have on the ^{15}N-isotope effect (*11*). Formation of a transition state proton bridge between the active site imidazolium moiety of His^{57} and the departing aniline is predicted to considerably reduce the magnitude of the nitrogen isotope effect for C−N bond fission from the theoretical maximum of 1.044 (*14*).

$(^{15}k_E)_{amido}$ for the α-CT-catalyzed hydrolysis of Suc-Phe-pNA is temperature independent and helps explain the convex Eyring plots that have been observed for this reaction (Figure 1). For enzyme-catalyzed reactions, there are two general explanations for convex Eyring plots (*1*): (i) partial rate limitation by two or more steps in a sequential, multistep reaction process and (ii) temperature-sensitive coupling of an enzyme conformational change to the chemical step of

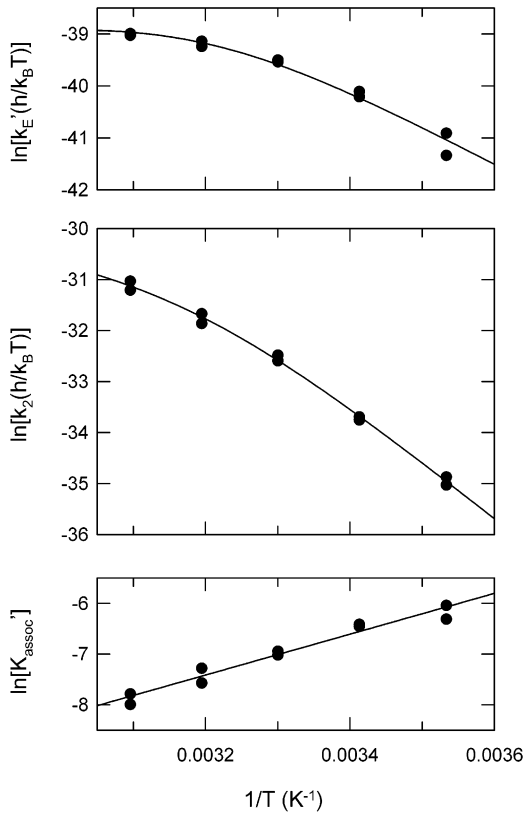

FIGURE 1: Temperature dependencies of steady-state kinetic parameters for the α-CT-catalyzed hydrolysis of Suc-Phe-pNA. pH-independent mechanistic parameters, k_E, k_2, and K_s were taken from the work of Case and Stein (*1*) and plotted here as dependencies on reciprocal temperature. In these plots, k_E is expressed as the product $k_E[E]_{standard-state}$ or k'_E, and K_s is expressed as the product $(K_s^{-1})[S]_{standard-state}$ or K'_{assoc} where the standard-state concentrations are set to 10^{-6} M. The line through the data sets for k'_E were drawn using the thermodynamic form of eq 18 and best-fit parameters: $\Delta H^{\neq}_{Ea} = 14.8 \pm 0.5$ kcal/mol and $\Delta S^{\neq}_{Ea} = 29.9 \pm 0.2$ e.u. with the constraints of $\Delta H^{\neq}_{\alpha} = 17.9$ kcal/mol and $\Delta S^{\neq}_{\alpha} = 57$ e.u. The line through the data sets for k_2 were drawn using the thermodynamic form of eq 7 and best-fit parameters: $\Delta H^{\neq}_{2a} = 22.4 \pm 3.7$ kcal/mol and $\Delta S^{\neq}_{2a} = 9.5 + 13.3$ e.u., and $\Delta H^{\neq}_{\alpha} = 17.9 \pm 7.3$ kcal/mol and $\Delta S^{\neq}_{\alpha} = 57.0 \pm 20.3$ e.u. The line through the data for K'_{assoc} was based on a simple van't Hoff plot with $\Delta H_{assoc} = -8.05 \pm 0.58$ kcal/mol and $\Delta S_{assoc} = -40.6 \pm 1.9$ e.u.

catalysis.[3] As we show below, our observation of temperature-independent ^{15}N-isotope effects for the α-CT-catalyzed hydrolysis of Suc-Phe-pNA allows elimination of the former alternative.

We start with the general mechanism of Scheme 2 and the observation that the data of Figure 1 for k_E and k_2 can be successfully fit to forms of eqs 7 and 18 which have been recast in thermodynamic form. Note that eq 18 is a simplified form of eq 8 in which, for reaction of α-CT with Suc-Phe-pNA and related substrates, $k_{-1} \gg k_{2a}$ (*1*).

$$k_E = \frac{k_{2a}/K_s}{1+\alpha} = \frac{k_{Ea}}{1+\alpha} \qquad (18)$$

The results of this fit indicate that according to the model

[3] Cast in mechanism-independent, thermodynamic terms, this amounts to a nonzero heat capacity of activation.

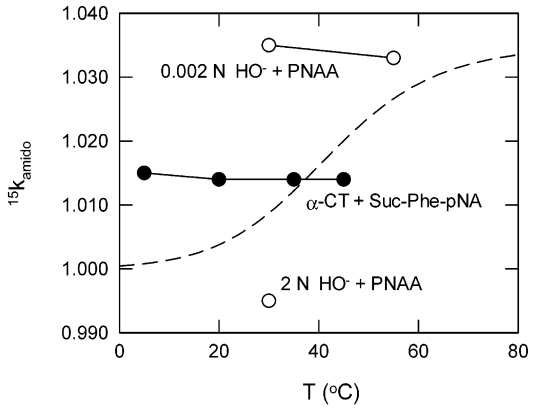

FIGURE 2: Temperature dependencies of ^{15}N-isotope effects for alkaline and α-CT-catalyzed hydrolysis of *p*-nitroanilides. The data points are from Table 1, while the dashed line was drawn using eq 17 and the temperature dependence of α (see legend of Figure 1) with $^{15}k^*_{2a}$ and $^{15}k^*_{2b}$ set equal to unity and 1.035, respectively.

of Scheme 2, at low temperature, $\alpha < 1$ and $k_2 = k_{2a}$, while at high temperature, $\alpha > 1$ and $k_2 = (k_{2a}/k_{-2a})k_b$.

Now, if this mechanism were to obtain, the ^{15}N-isotope effect would display a significant temperature dependence. This is illustrated in Figure 2 which displays the temperature dependence of $^{15}k_{amido}$ for a hypothetical case based on eq 17 and the temperature dependence of α (see legend of Figure 1) with $^{15}k^*_{2a}$ and $^{15}k^*_{2b}$ set equal to unity and 1.035, respectively. Other reasonable values for $^{15}k^*_{2a}$, which might range from 0.99 to 1.005, and $^{15}k^*_{2b}$, which might range from 1.010 to 1.045, give no better fit to the temperature-independent ^{15}N-isotope effects for this reaction. On the basis of this analysis, it is clear that the curved Eyring plots of Figure 1 and related α-CT-catalyzed reactions (*1*) do not originate from a mechanism involving a temperature-dependent change in rate-limiting step.

The other mechanistic alternative involves the coupling of conformational isomerizations of α-CT to the chemistry that occurs during transformation of the Michaelis complex to acyl-enzyme (*1*). While the idea that protein conformational changes can be directly coupled to active site chemistry to enhance enzyme catalytic efficiency is not a new one (*15*−*19*), interest in it has recently been renewed with the observation of the apparent coupling of protein motions to active site hydrogen tunneling in a number of hydrogen transfer reactions (*20*, *21*).

The specific model that Case and Stein (*1*) advanced previously to explain the convex Eyring plots for acylation of α-CT by specific substrates is a thermodynamic model summarized in eq 19:

$$\Delta G^{\neq}_c = \Delta G^{\neq}_{chem} - \gamma(\Delta G^{\neq}_{chem} - \Delta G^{\neq}_{isom}) \qquad (19)$$

where $\Delta G^{\neq}_c$, the energy of activation for the process governed by k_c, is a function of $\Delta G^{\neq}_{chem}$, the energy of activation for the chemical conversion that occurs in the absence of any protein conformational change, and $\Delta G^{\neq}_{isom}$, the energy of activation for the protein isomerization that occurs in the absence of chemistry. γ is the coupling constant and can range from 0 to 1.

We see from this expression that coupling of chemistry to a conformational fluctuation of the protein allows the rate

of the chemical process to increase by a factor that is related to the free energy difference between uncoupled active site chemistry and conformational isomerization. In the limiting situation in which there is no coupling ($\gamma = 0$), turnover of the Michaelis complex proceeds inefficiently and with a rate constant k_c that equals k_{chem}. Protein conformational changes may of course also occur, but since these are uncoupled to chemistry they cannot act to increase the magnitude of k_c. Now, in situations in which coupling occurs, chemistry and protein isomerization comprise a single, concerted process that is governed by the single rate constant k_c, which necessarily is larger than k_{chem} but smaller than k_{isom}. If coupling is perfectly efficient ($\gamma = 1$), k_c becomes equal in magnitude to the limiting value, k_{isom}. If coupling is viewed from the point of view of active site chemistry, it appears that as coupling efficiency increases, the rate constant for chemistry increases at the expense of protein isomerization, finally to equal k_{isom} in the case of perfect coupling.

Significant questions remain concerning the nature of coupling and how it can be described and explained in terms of protein chemical/structural determinants. At least for α-CT, it appears that coupling efficiency is at least partly determined by structural features of the substrate and increases with increasing chain length of peptide substrates (*1*). It remains a challenge to understand how occupancy of active site subsites on α-CT, and perhaps other serine proteases, leads to more efficacious coupling and enhanced reaction rates. Specifically in the context of this model, we need to understand γ and whether it is temperature dependent, a condition that is necessary if we are to explain the convex Eyring plots which motivated this work.

The above analysis of coupling of chemistry and protein conformational isomerizations stemmed from our observation of temperature-independent ^{15}N-isotope effects on the α-CT-catalyzed hydrolysis of Suc-Phe-pNA. But what is remarkable is that this temperature independence is absolute, that is, there is no statistically significant change in $^{15}(k_E)_{amido}$ over the temperature range from 5° and 45 °C (see Table 1). Over this increase in temperature, one can calculate, strictly using zero-point energy considerations, a decrease in the ^{15}N-isotope effect of 0.3−0.4%. And this is just what we see for the alkaline hydrolysis of PNAA in 0.002 N hydroxide. Here one calculates and observes a 0.2% decrease in $^{15}k_{amido}$ from 1.035 to 1.033 as the temperature increases from 30 to 55 °C. The near temperature independence of ^{15}N-isotope effect on the enzymatic reaction is unexpected, and to our knowledge unprecedented, but may reflect properties of a unique transition state for this process in which we have postulated coupling of protein dynamics with active site chemistry.

REFERENCES

1. Case, A., and Stein, R. L. (2003) Mechanistic Origins of the Substrate Selectivity of Serine Proteases. *Biochemistry 42*, 3335−3348.
2. Bigeleisen, J. (1958) Theoretical and Experimental Aspects of Isotope Effects in Chemical Kinetics. *Adv. Chem. Phys. 1*, 15−76.
3. Rao, M., Barlow, P. N., Pryor, A. N., Paneth, P., O'Leary, M. H., Quinn, D. M., and Huskey, P. (1993) Nitrogen Isotope Effects on Acetylcholinesterase-Catalyzed Hydrolysis of *o*-Nitroacetanilide. *J. Am. Chem. Soc. 115*, 11676−11681.
4. Schowen, R. L. (1978) in *Transition States of Biochemical Processes* (Gandour, R. D., Schowen, R. L., Eds.) pp 77−114, Plenum Press, New York.
5. Hengge, A. C., and Cleland, W. W. (1990) Direct Measurement of Transition-State Bond Cleavage in Hydrolysis of Phosphate Esters of *p*-Nitrophenol. *J. Am. Chem. Soc. 112*, 7421−7422.
6. Stein, R. L., Fujihara, H., Quinn, D. M., Fischer, G., Kuellertz, G., Barth, A., and Schowen, R. L. (1984) Transition-State Structural Features for Anilide Hydrolysis from β-Deuterium Isotope Effects. *J. Am. Chem. Soc. 106*.
7. Huskey, W. P. (1991) in *Enzyme Mechanism from Isotope Effects* (Cook, P. F., Ed.) pp 37−72, CRC Press, Boca Raton, FL.
8. Melander, L., and Saunders, W. H. (1980) in *Reaction Rates of Isotopic Molecules*, pp 172−174, Wiley, New York.
9. O'Leary, M. H., and Kluetz, M. D. (1970) Identification of the Rate-Limiting Step in the Chymotrypsin-Catalyzed Hydrolysis of N-Actyl-L-Tryptophanamide. *J. Am. Chem. Soc. 92*, 6089−6090.
10. O'Leary, M. H., Urberg, M., and Young, A. P. (1974) Nitrogen Isotope Effects on the Papain-Catalyzed Hydrolysis of N-Benzoyl-L-Argininamide. *Biochemistry 13*, 2077−2081.
11. Hengge, A. C. (2002) Isotope Effects in the Study of Phosphoryl and Sulfuryl Transfer Reactions. *Acc. Chem. Res. 35*, 105−112.
12. Stein, R. L. (1981) Analysis of Kinetic Isotope Effects on Complex Reactions Utilizing the Concept of the Virtual Transition State. *J. Org. Chem. 46*, 3328−3330.
13. O'Leary, M. H., and Kluetz, M. D. (1972) Nitrogen Isotope Effects on the Chymotrypsin-Catalyzed Hydrolysis of N-Acetyl-L-Tryptophanamide. *J. Am. Chem. Soc. 94*, 3585−3589.
14. Rishavy, M. A., and Cleland, W. W. (1999) ^{13}C, ^{15}N, ^{16}O Equilibrium Isotope Effects and Fractionation Factors. *Can. J. Chem. 77*, 967−977.
15. Lumry, R., and Biltonen, R. (1969) in *Structure and Stability of Biological Macromolecules* (Timasheff, S., and Fasman, G., Eds.) Chapter 2, Dekker, New York.
16. Careri, G., Fasella, P., and Gratton, E. (1979) Enzyme Dynamics: The Statistical Physics Approach. *Annu. Rev. Biophys. Bioeng. 8*, 69−97.
17. Welch, G. R., Somogyi, B., and Damjanovic, S. (1982) The Role of Protein Fluctuations in Enzyme Action: A Review. *Prog. Biophys. Mol. Biol. 39*, 109−146.
18. Somogyi, B., Welch, G. R., and Damjanovic, S. (1984) The Dynamic Basis of Energy Transduction in Enzymes. *Biochim. Biophys. Acta 768*, 81−112.
19. Welch, G. R. (1986) *The Fluctuating Enzyme*, John Wiley & Sons, New York.
20. Antoniou, D., Caratzoulas, S., Kalyanaraman, C., Mincer, J. S., and Schwartz, S. D. (2002) Barrier Passage and Protein Dynamics in Enzymatically Catalyzed Reactions. *Eur. J. Biochem. 269*, 3102−3112.
21. Knapp, M. J., and Klinman, J. P. (2002) Environmentally Coupled Hydrogen Tunneling − Linking Catalysis to Dynamics. *Eur. J. Biochem. 269*, 3113−3121.

BI030222K